Journal of Magnetic Resonance **144,** 207–216 (2000)
doi:10.1006/jmre.2000.2045, available online at http://www.idealibrary.com on IDEAL®

Deuterium Nuclear Spin–Lattice Relaxation Times and Quadrupolar Coupling Constants in Isotopically Labeled Saccharides

Bidisha Bose-Basu,* Jaroslav Zajicek,* Gail Bondo,† Shikai Zhao,† Meredith Kubsch,† Ian Carmichael,‡ and Anthony S. Serianni*,[1]

*Department of Chemistry and Biochemistry, University of Notre Dame, Notre Dame, Indiana 46556; †Omicron Biochemicals, Inc., 1347 North Ironwood Drive, South Bend, Indiana 46615-3566; and ‡Radiation Laboratory, University of Notre Dame, Notre Dame, Indiana 46556

Received July 30, 1999; revised January 18, 2000

^{13}C and ^{2}H spin–lattice relaxation times have been determined by inversion recovery in a range of site-specific ^{13}C- and ^{2}H-labeled saccharides under identical solution conditions, and the data were used to calculate deuterium nuclear quadrupolar coupling constants (^{2}H NQCC) at specific sites within cyclic and acyclic forms in solution. ^{13}C T_1 values ranged from ~0.6 to 8.2 s, and ^{2}H T_1 values ranged from ~79 to 450 ms, depending on molecular structure (0.4 M sugar in 5 mM EDTA (disodium salt) in $^{2}H_2O$-depleted H_2O, pH 4.8, 30°C). In addition to providing new information on ^{13}C and ^{2}H relaxation behavior of saccharides in solution, the resulting ^{2}H1 NQCC values reveal a dependency on anomeric configuration within aldopyranose rings, whereas ^{2}H NQCC values at other ring sites appear less sensitive to configuration at C1. In contrast, ^{2}H NQCC values at both anomeric and nonanomeric sites within aldofuranose rings appear to be influenced by anomeric configuration. These experimental observations were confirmed by density functional theory (DFT) calculations of ^{2}H NQCC values in model aldopyranosyl and aldofuranosyl rings. © 2000 Academic Press

Key Words: **^{2}H T_1; ^{13}C T_1; ^{2}H quadrupolar coupling constants; isotopically labeled saccharides.**

INTRODUCTION

^{2}H Nuclear spin-relaxation times are useful NMR parameters in investigations of molecular motion and exchange processes in solution (*1–3*). Since the only significant contribution to ^{2}H relaxation arises from the motional modulation of the interaction between the quadrupole moment and the electric field gradient at the nucleus, the interpretation of ^{2}H relaxation is less prone to error, in comparison to ^{1}H and ^{13}C relaxation, where multiple relaxation mechanisms occur (*4*). In addition, unlike ^{13}C relaxation, cross-relaxation and cross-correlation mechanisms have been found to be negligible for ^{2}H, thus further simplifying their interpretation in motional terms.

^{2}H spin–lattice relaxation (^{2}H T_1) in molecules tumbling isotropically in the region of extreme motional narrowing is described by

$$1/T_{1D} = 3/8(1 + \eta^2/3)(e^2qQ/\hbar)^2\tau_D, \qquad [1]$$

where $1/T_{1D}$ is the ^{2}H spin–lattice relaxation rate, η is the asymmetry parameter of the field gradient, e^2qQ/h is the ^{2}H nuclear quadrupolar coupling constant (NQCC), and τ_D is the overall rotational correlation time for the C–^{2}H bond. For a C–^{2}H fragment, the asymmetry parameter is considered to be very small or zero, and therefore it is often ignored. Thus, with a knowledge of ^{2}H NQCC, ^{2}H T_1 can be related to τ_D and thus to molecular motion in solution.

Nuclear quadrupolar coupling constants have been shown to contain useful structural information. For example, ^{2}H NQCC values in O–^{2}H ··· O systems are sensitive to the O–O internuclear distance, and thus to the strength of the hydrogen-bonding interaction (*5*). The main determinant of the field gradient at ^{2}H is not the electrons in the hydrogen 1*s* orbital but the nucleus to which it is directly bonded and the electrons donated by this nucleus (*6*). As a consequence, ^{2}H NQCC report on the electronic environment of deuterium nuclei in the ground state, leading to the expectation that ^{2}H NQCC might be sensitive to electronic differences at the anomeric carbon of saccharides where stereoelectronic factors are known to play an important role, or possibly at O–^{2}H groups involved in hydrogen-bonding to solvent or other solutes. ^{2}H NQCC values are expected to depend on C–^{2}H bond length (*7*), and thus their measurement in carbohydrate systems where C–H bond length changes have been reported, could be valuable.

Despite these and other advantages, very little data on ^{2}H spin–lattice relaxation times and quadrupolar coupling constants in saccharides have been reported. This investigation describes solution measurements of these parameters in cyclic and acyclic saccharides that have been site-specifically labeled with ^{2}H at anomeric and nonanomeric methine carbons. In order to calculate ^{2}H NQCC values in solution, complementary ^{13}C T_1 measurements were made using site-specifically ^{13}C-labeled compounds; these relaxation data are interpreted qualitatively in terms of saccharide structure and conformation. Calculations of ^{2}H NQCC values using density functional theory (DFT) have also been performed in aldopyranose and aldofuranose models to test the experimental findings.

[1] To whom correspondence should be addressed. E-mail: serianni.1@nd.edu.

1090-7807/00 $35.00

EXPERIMENTAL

Preparation of ^{13}C- and ^{2}H-Labeled Compounds

D-[1-^{13}C]Galactose, D-[2-^{13}C]galactose, D-[1-^{13}C]glucose, D-[2-^{13}C]glucose, D-[3-^{13}C]glucose, D-[5-^{13}C]glucose, D-[1-^{13}C]mannose, D-[2-^{13}C]mannose, D-[1-^{13}C]arabinose, D-[2-^{13}C]arabinose, D-[1-^{13}C]lyxose, D-[1-^{13}C]ribose, D-[2-^{13}C]ribose, D-[1-^{13}C]xylose, D-[2-^{13}C]xylose, D-[1-^{13}C]erythrose, DL-[1-^{13}C]glyceraldehyde, [1-^{13}C]glycolaldehyde, and [1-^{13}C^{glc}]lactose (Scheme 1) were prepared by methods described previously (*8–12*).

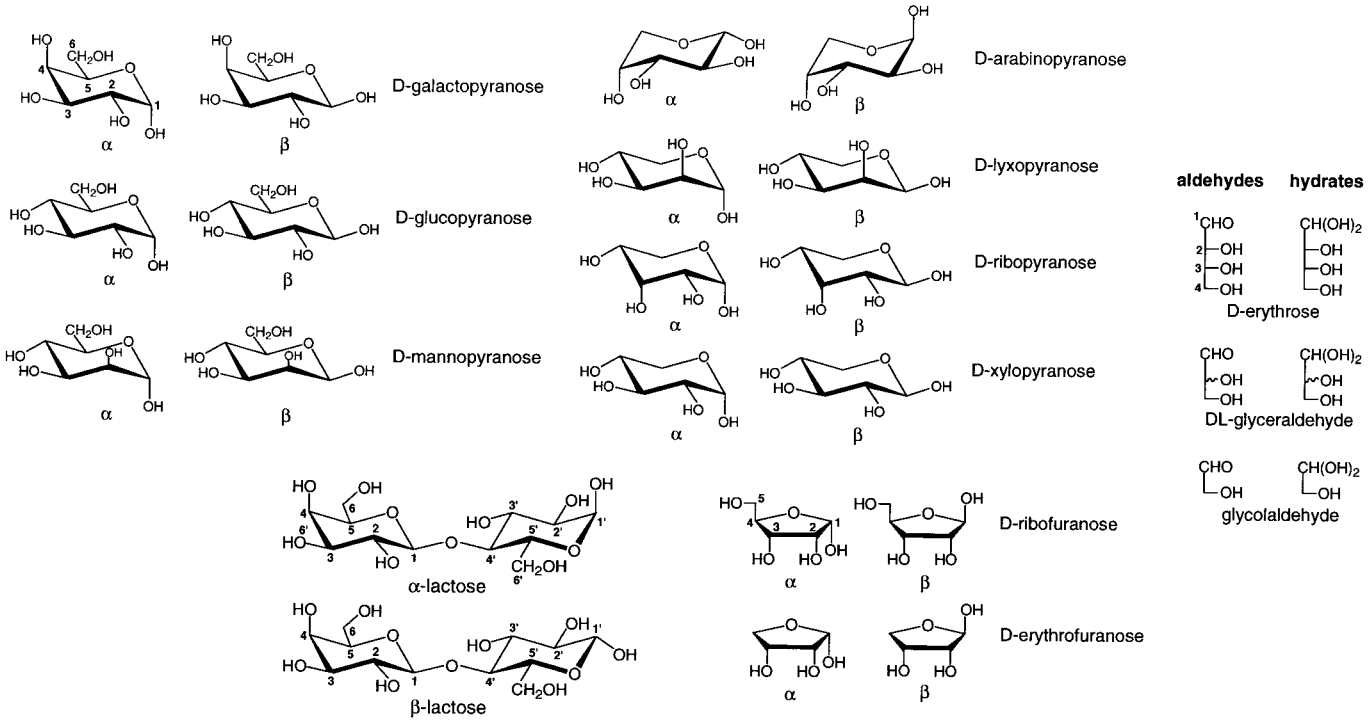

SCHEME 1

D-[1-^{2}H]Galactose, D-[2-^{2}H]galactose, D-[1-^{2}H]glucose, D-[2-^{2}H]glucose, D-[3-^{2}H]glucose, D-[5-^{2}H]glucose, D-[1-^{2}H]mannose, D-[2-^{2}H]arabinose, D-[1-^{2}H]lyxose, D-[1-^{2}H]ribose, D-[2-^{2}H]ribose, D-[1-^{2}H]xylose, D-[2-^{2}H]xylose and DL-[1-^{2}H]glyceraldehyde (Scheme 1) were prepared as described previously (*13, 14*).

Spin–Lattice Relaxation Time (T_1) Determinations

^{13}C and ^{2}H T_1 values were determined as follows. Pairs of site-specifically labeled compounds (one ^{13}C-labeled and one ^{2}H-labeled; e.g., D-[1-^{13}C]glucose and D-[1-^{2}H]glucose) were dissolved in an EDTA (disodium salt) solution (5 mM, pH 4.8) prepared using ^{2}H-depleted H_2O (Sigma) to give a final 0.2 M concentration of each compound (total saccharide concentration, 0.4 M). Prior to each T_1 determination, the solution was degassed with argon for 3–4 min in a 3-mm NMR tube, and the tube was sealed with a plastic cap.

Spin–lattice relaxation times (T_1) were measured by inversion-recovery (*15*) with a 180° composite pulse on a Varian Unity*Plus* 600 MHz NMR spectrometer operating at 150.840 MHz for ^{13}C and 92.085 MHz for ^{2}H and using a 3-mm microprobe (Nalorac). Sample temperature was regulated at 30°C. All determinations were made with the spectrometer in an unlocked mode. Relaxation delays were chosen to be at least 10 times the longest T_1 in the sample, and 15–21 τ values, distributed as recommended previously (*16*), were used to define the relaxation curve. For a given sample, a minimum of five T_1 determinations were made on each nucleus, and peak intensity data were fit nonlinearly (3-parameter) using software supplied by Varian Instruments. The computed ^{13}C and ^{2}H T_1 values were averaged and used to calculate ^{2}H NQCC values.

Experimental Calculations of Deuterium Nuclear Quadrupolar Coupling Constants (^{2}H NQCC)

^{2}H NQCC values were calculated indirectly from independent measurements of ^{13}C and ^{2}H spin–lattice relaxation times (*17*) and were restricted to ^{2}H nuclei on methine carbons. In the compounds examined, rapid overall isotropic reorientation

($\omega^2\tau_c^2 \ll 1$) and dipole–dipole relaxation for ^{13}C were assumed (*18, 19*), thus permitting use of (*4*)

$$1/T_{1C} = N\hbar^2\gamma_C^2\gamma_H^2 r_{CH}^{-6}\tau_{CH}, \qquad [2]$$

where $1/T_{1C}$ is the ^{13}C spin–lattice relaxation rate, N is the number of protons attached to the carbon ($N = 1$ in this investigation), $\hbar$ is Planck's constant divided by 2π, γ_H and γ_C are the gyromagnetic ratios of ^{1}H and ^{13}C, respectively, r_{CH} is the C–H bond length, and τ_{CH} is the overall rotational correlation time for the C–H bond. Equations [1] and [2] were combined to give (*1*),

$$8\gamma_H^2\gamma_C^2 T_{1C}\hbar^2/3r_{CH}^6 T_{1D} = [e^2qQ/\hbar]^2, \qquad [3]$$

which was used to calculate ^{2}H NQCC values. A C–H bond length of 1.08×10^{-8} m (1.08 Å) was used in all calculations. The use of Eq. [3] assumes that τ_{CH} and τ_D are identical, that is, there is no isotope effect on correlation times in the systems examined.

Theoretical Calculations of Deuterium Nuclear Quadrupolar Coupling Constants (^{2}H NQCC)

Molecular orbital calculations were performed with a modified (*20*) version of the Gaussian 94 suite of programs (*21*) on the aldopentopyranose models **1** and **2** and aldopentofuranose model **3**.

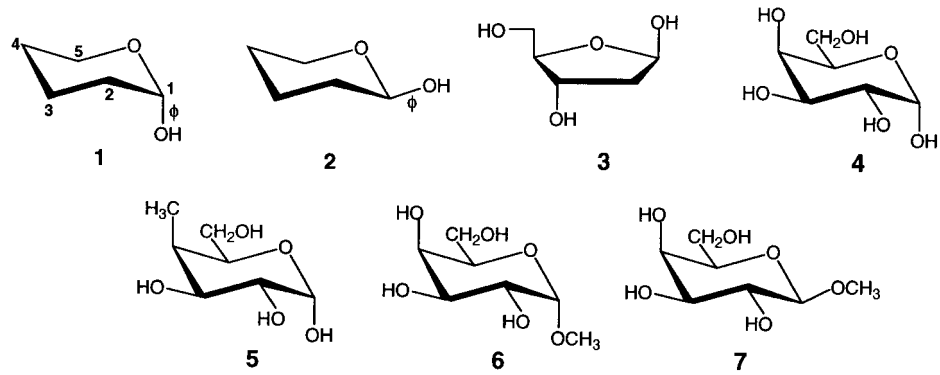

Electron correlation effects were treated by means of density functional theory (DFT) using the standard B3LYP functional described by Becke (*22*). This functional comprises both local (*23*) and nonlocal (*24*) exchange contributions and contains terms accounting for local (*25*) and nonlocal (*26*) correlation corrections. Geometric optimizations were conducted with the B3LYP functional and the standard split-valence 6-31G* basis set (*27*). The ϕ glycosidic torsion angle in **1** and **2**, defined as H1–C1–O1–H, was set initially at $-60°$ (OH1 gauche to H1 and O5), which is the expected most stable conformation based on stereoelectronic and steric considerations (*28*). Calculations on **3** were conducted on each envelope conformation (10 structures) using methods and initial exocyclic torsion angles described previously (*29*). ^{2}H NQCC values were calculated in geometrically optimized **1**–**3** using the B3LYP functional and a [5*s*2*p*1*d*,3*s*1*p*] basis set.

RESULTS AND DISCUSSION

Motional Models and Reliability of T_1 Determinations

Relaxation data obtained on all compounds were treated with the assumption that overall molecular reorientation in solution is isotropic (i.e., Eqs. [1]–[3]). Previous relaxation studies of simple monosaccharides have confirmed this behavior (*18, 19*). Qualitative analysis of ^{13}C relaxation data in methyl β-D-aldopyranosides have suggested slight motional anisotropy caused by an effect of the CH_3 substituent on the inertial axes sufficient to cause molecular diffusion about a preferred, but undefined, axis of rotation (*30*). These effects were not observed in methyl α-D-aldopyranosides. This study was, therefore, confined to reducing sugars, thus eliminating potential problems arising from the presence of an aglycone. In addition, relaxation measurements were limited to ring nuclei only; nuclei located on hydroxymethyl groups were not examined due to complications arising from internal motions superimposed on overall motional reorientation.

Previous studies (*16*) identified key factors that affect the accuracy and precision of T_1 measurements made by inversion recovery (*15*). The distribution of data points along the relaxation curve is an important variable; in this study, 15–21 τ values were used, and these values were distributed in accordance with previous recommendations (*16*). Five measurements of each T_1 were made and the data were averaged to give the final average $T_1 \pm 1$ STD (Fig. 1). The relaxation data were fit nonlinearly to extract T_1s, which has been shown to be superior to a linear fit of the data.

To evaluate the reproducibility of the T_1 determinations, ^{13}C and ^{2}H T_1 values were measured on the *same* sample contain-

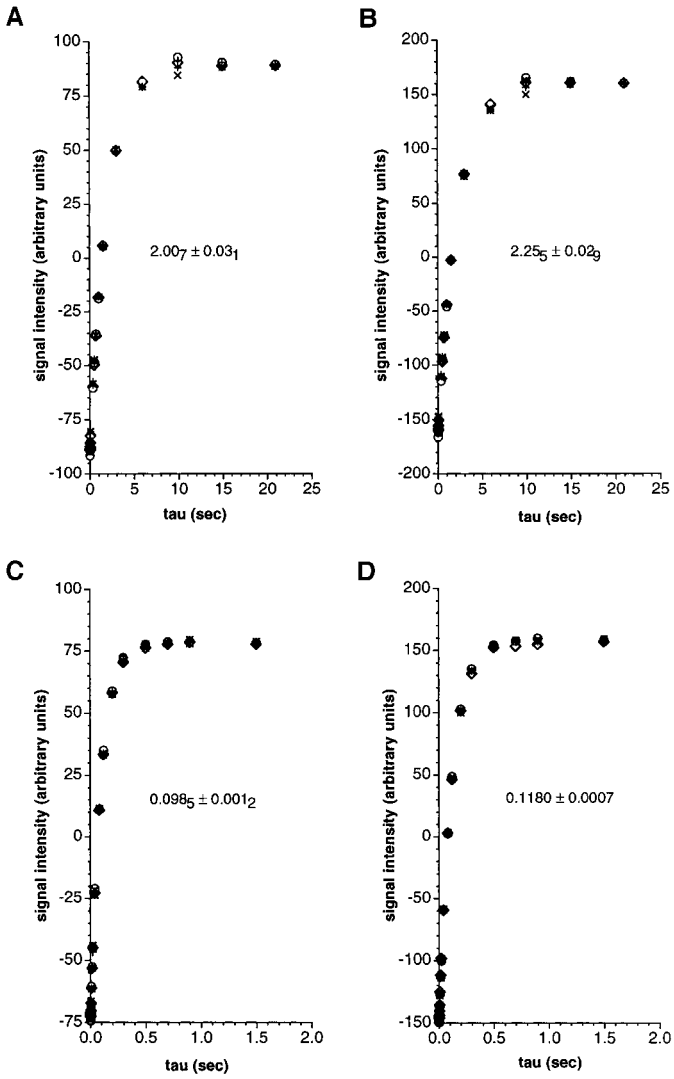

FIG. 1. Inversion–recovery T_1 relaxation data obtained on a 50:50 mixture of D-[1-^{13}C]xylose and D-[1-^{2}H]xylose (0.4 M) in 5 mM EDTA (disodium salt) in $^{2}H_2O$-depleted H_2O, pH. 4.8, 30°C. Five independent data sets were obtained to calculate ^{13}C and ^{2}H T_1 values for the labeled sites within both pyranoses. (A) ^{13}C relaxation, α-xylopyranose: 2.005, 2.016, 2.033, 2.025, 1.954 s. (B) ^{13}C relaxation, β-D-xylopyranose: 2.252, 2.248, 2.286, 2.278, 2.213 s. (C) ^{2}H relaxation, α-D-xylopyranose: 0.09911, 0.09654, 0.09978, 0.09854, 0.09831 s. (D) ^{2}H relaxation, β-D-xylopyranose: 0.1174, 0.1176, 0.1185, 0.1189, 0.1174 s. The value shown in each plot is the average T_1 calculated from the five data sets ± 1 STD.

ing a 50:50 mixture of D-[1-^{13}C]xylose:D-[1-^{2}H]xylose, under the solution conditions described in Experimental on two separate occasions. In addition, ^{13}C T_1 values were determined on two *different* samples of a 50:50 mixture of D-[1-^{13}C]ribose: D-[1-^{2}H]ribose. The results are summarized in Table 1. The excellent reproducibility validates the methodology used to determine T_1 values and permits an evaluation of the error associated with ^{2}H NQCC determined from them.

Spin–Lattice Relaxation Times

The ^{13}C T_1 values measured in this investigation (Table 1) exhibit the expected dependence on molecular size (*31*), with longer T_1s associated with smaller molecules. Thus, for example, under identical solution conditions, $T_{1,C1}$ values for [1-$^{13}C^{glc}$]lactose (MW 343 D) were 0.57 s (α) and 0.73 s (β), whereas $T_{1,C1}$ values for [1-^{13}C]glycolaldehyde were 5.74 s (hydrate; MW 79 D) and 8.20 s (aldehyde; MW 61 D).

The average spin–lattice relaxation rate, $1/T_1$, for aldohexopyranoses (16 values) was 0.68 ± 0.03 s^{-1}, whereas that of aldohexofuranoses (4 values) was 0.55 ± 0.01 s^{-1}, suggesting different motional properties in these two ring structures. By comparison, the average $1/T_1$ for aldopentopyranoses (14 values, 0.45 ± 0.03 s^{-1}) and aldopentofuranoses (4 values, 0.42 ± 0.03 s^{-1}) are indistinguishable, suggesting that the motional properties of these two types of structures are similar. We assume that differences in C–H bond lengths are small and can be neglected in the above comparisons. $1/T_{1,avg}$ for aldohexopyranoses and aldopentopyranoses differ by 0.23 s^{-1}, and for aldopentofuranoses and aldotetrofuranoses by 0.20 s^{-1}. Thus, a change in mass of 30 D (addition/removal of a HCOH fragment) translates into a ~0.22 s^{-1} change in ^{13}C relaxation rate.

In the erythrofuranoses, $1/T_{1,avg}$ = 0.22 s^{-1}, whereas values of 0.21 and 0.42 s^{-1} are observed for erythrose aldehyde and hydrate, respectively. The larger value for the hydrate is partly attributed to its higher mass, but correcting for this contribution ([0.22 s^{-1}] × 18⁄30 = 0.13 s^{-1}) gives a residual rate of 0.07 s^{-1}. Since it is unlikely that this residual is caused by different C1–H1 bond lengths, its origin is attributed to a more extended conformation of the acyclic hydrate relative to the furanoses (*31*), increased interactions with solvent water (greater molecular "friction") caused by additional free OH groups in the hydrate, and/or possible motional anisotropy. Interestingly, $1/T_1$ of the aldehyde and furanose forms are nearly identical. C1–H1 bond length differences might be expected here, with a slightly shorter bond in the aldehyde. This effect, if present, is apparently offset by conformational factors, altered hydrogen bonding with solvent and/or motional anisotropy. Unlike the hydrate, the aldehyde might assume a pseudocyclic or bent conformation in solution, thus mimicking the cyclic furanose with respect to overall motion. Since relaxation measurements were made on the same solution, solution viscosity cannot be an influencing factor.

Differences in $1/T_1$ between the aldehyde and hydrate forms of DL-[1-^{13}C]glyceraldehyde and [1-^{13}C]glycolaldehyde are 0.12 and 0.05 s^{-1}, respectively. The former is attributed to the mass difference, but the latter falls short based on mass considerations alone. The latter finding suggests that the value of ~0.22 s^{-1}/30 amu, derived from the examination of cyclic structures, is not applicable to a wide range of molecular structures and masses. Indeed, a plot of $1/T_1$ vs molecular mass using all of the available data is nonlinear over the mass range examined (Fig. 2). The resolution of Fig. 1 into aldehyde,

TABLE 1
^{13}C Spin–Lattice Relaxation Times[a] in Various Carbohydrates

Compound	α-pyranose	β-pyranose	α-furanose	β-furanose	Hydrate	Aldehyde
lactose						
C1	0.565 ± 0.003	0.725 ± 0.004				
D-galactose						
C1	1.515 ± 0.003	$1.54_7 \pm 0.03_7$	$1.75_1 \pm 0.01_1$	$1.84_7 \pm 0.01_3$		
C2	$1.50_2 \pm 0.02_0$	$1.50_8 \pm 0.02_3$	$1.82_8 \pm 0.02_3$	$1.81_7 \pm 0.02_9$		
D-glucose						
C1	$1.42_4 \pm 0.01_4$	$1.51_3 \pm 0.01_5$				
C2	$1.48_5 \pm 0.03_2$	$1.45_8 \pm 0.01_7$				
C3	$1.47_2 \pm 0.02_6$	$1.46_6 \pm 0.02_5$				
C5	$1.49_5 \pm 0.01_5$	$1.49_3 \pm 0.00_8$				
D-mannose						
C1	$1.39_5 \pm 0.01_6$	$1.54_0 \pm 0.02_1$				
C2	1.312 ± 0.005	1.390 ± 0.008				
D-arabinose						
C1	$2.36_6 \pm 0.04_3$	$2.34_5 \pm 0.03_7$	$2.60_1 \pm 0.04_6$	$2.53_9 \pm 0.03_4$		
C2	$2.25_2 \pm 0.03_0$	$2.23_4 \pm 0.02_1$				
D-lyxose						
C1	$2.0_4 \pm 0.1_5$	$2.34_5 \pm 0.05_1$				
D-ribose						
C1 (exp 1)[b]	$2.49_7 \pm 0.01_2$	$2.33_4 \pm 0.02_3$	$2.50_2 \pm 0.01_8$	$2.29_4 \pm 0.02_1$		
C1 (exp 2)[b]	$2.61_6 \pm 0.01_4$	$2.44_5 \pm 0.01_4$	$2.64_5 \pm 0.03_0$	$2.38_8 \pm 0.02_9$	$1.57_1 \pm 0.09_0$	
C2	2.653 ± 0.004	$2.27_1 \pm 0.01_8$	$2.56_3 \pm 0.01_9$	$2.25_2 \pm 0.03_0$		
D-xylose						
C1 (exp 1)[c]	$2.00_7 \pm 0.02_1$	$2.26_6 \pm 0.03_1$				
C1 (exp 2)[c]	$2.00_7 \pm 0.03_1$	$2.25_5 \pm 0.02_9$				
C2	$2.25_1 \pm 0.02_3$	$2.19_0 \pm 0.01_2$				
D-erythrose						
C1			$4.6_9 \pm 0.2_4$	$4.5_1 \pm 0.1_1$	$2.4_0 \pm 0.1_3$	$4.7_2 \pm 0.1_7$
DL-glyceraldehyde						
C1					$3.38_6 \pm 0.08_9$	$5.7_0 \pm 0.1_9$
glycolaldehyde						
C1					$5.73_6 \pm 0.08_2$	$8.2_0 \pm 0.1_7$

[a] In seconds.
[b] Different samples.
[c] Same sample.

hydrate, and cyclic groups (Fig. 3) reveals possible differences in slopes, with the steepest associated with cyclic structures and the shallowest associated with acyclic aldehydes. These results imply that overall molecular structure significantly affects the relationship between molecular mass and rotational correlation time; molecular mass is not the only factor controlling the rate of molecular reorientation in solution of saccharides. The number and distribution of polar groups, and thus the nature of solute–solvent interactions, also influence overall correlation times. Thus, for example, even though the molecular masses of structures **4** and **5** are nearly identical, their relaxation properties are expected to differ due to altered interactions with solvent water.

^{2}H spin–lattice relaxation times (Table 2) are considerably shorter than ^{13}C T_1s under identical solution conditions. ^{2}H T_1 values range from 0.07 to 0.13 s for aldohexopyranoses, aldopentopyranoses, and aldopentofuranoses. These values increase considerably with decreasing molecular mass; thus, for example, ^{2}H T_1 values for DL-[1-^{2}H]glyceraldehyde hydrate and aldehyde are 0.17 and 0.45 s, respectively.

Deuterium Nuclear Quadrupolar Coupling Constants

^{2}H NQCC values, computed from Eq. [3] using the relaxation data in Tables 1 and 2, are given in Table 3. The reproducibility of these couplings was tested by determining the ^{2}H NQCC for α- and β-D-[1-^{2}H]xylopyranoses on two separate occasions. The computed values were as follows: α-pyranose, 176.8 and 176.7 kHz; β-pyranose, 171.5 and 171.2 kHz. These and other considerations (see further discussion below) indicate that the reported ^{2}H NQCC in Table 3 are accurate to within ± 1.0 kHz.

^{2}H NQCC values in aldofuranosyl and aldopyranosyl rings range from 172.2 to 178.9 kHz (Table 3). The ^{2}H NQCC for ^{2}H1 of DL-[1-^{2}H]glyceraldehyde hydrate (175.6 kHz) is similar to that for ^{2}H1 of [1-^{2}H]aldofuranoses and [1-^{2}H]aldopy-

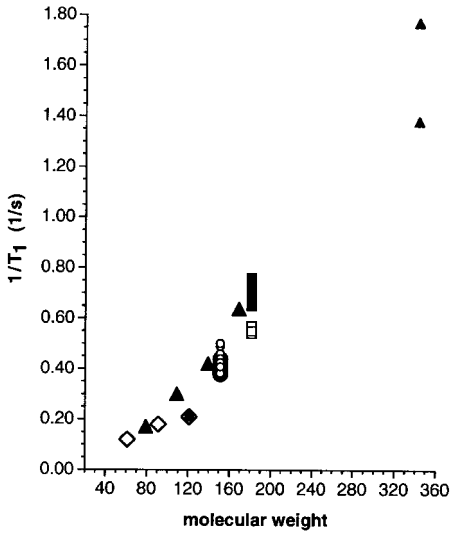

FIG. 2. The dependence of ^{13}C spin–lattice relaxation rate (T_1^{-1}) on saccharide molecular weight as determined from T_1 data given in Table 1. Closed squares represent aldohexopyranoses, open squares represent aldohexofuranoses, open circles represent aldopentopyranoses, closed circles represent aldopentofuranoses, closed diamonds represent aldotetrofuranoses, open diamonds represent aldehydes, small closed triangles represent disaccharides, and large closed triangles represent hydrates.

ranoses. In contrast, the ^2H NQCC for $^2H1$ of DL-[1-^2H]glyceraldehyde aldehyde is significantly smaller (139.2 kHz).

Within the aldohexopyranoses, a significant difference in NQCC values for $^2H1$ is observed between anomers, with α-pyranoses (which contain an equatorial C1–$^2H1$ bond) consistently yielding the larger coupling. This pattern is not observed at nonanomeric carbons; for example, the NQCC for $^2H1$ in *gluco* anomers differ by 5.8 kHz, whereas those for $^2H2$, $^2H3$, and $^2H5$ differ by 0.5–1.7 kHz. The origin of the effect at $^2H1$ may be related to different C–^2H bond lengths between anomers. To evaluate this factor, the effect of C1–H1 bond length on ^2H NQCC for $^2H1$ in α-D-glucopyranose was calculated using the ^{13}C and ^2H T_1 data in Tables 1 and 2. A plot of NQCC as a function of $r_{C1,H1}$ (Fig. 4) is nearly linear for $r_{C1,H1}$ values ranging from 1.05 to 1.12 Å, with NQCC decreasing by ~5 kHz per 0.01 Å increase in C–H bond length. It is important to note that, in the determination of NQCC values shown in Table 3, *equal* C1–H1 bond lengths in the α- and β-pyranoses were assumed (1.08 Å). If C1–H1 bond lengths differ between anomers, it is more likely that the equatorial bond (α-pyranose) would be *shorter* than the axial bond (β-pyranose), but a difference of no more than 0.01 Å is expected. If the C1–H1 bond in α-D-glucopyranose is thus assumed to be 0.01 Å shorter than that in β-D-glucopyranose (i.e., 1.07 Å), the recalculated ^2H NQCC in the α-pyranose increases to 184.0 kHz, thus further enhancing the difference in NQCC values between anomers. Thus, the method used to calculate NQCC values in Table 3 would underestimate the difference in NQCC between anomers. The data, therefore, suggest that NQCC for $^2H1$ depend on anomeric configuration, with larger values predicted for α-pyranoses, but the magnitude of the difference cannot be quantified accurately using the present experimental method.

Given the above experimental limitations, ^2H NQCC values were computed from density functional theory (DFT) in two model aldopyranoses **1** and **2**, which mimic α- and β-pyranoses, respectively. Computed C–H bond lengths and theoretical ^2H NQCC values are reported in Table 4. The computed couplings are in qualitative agreement with experimental data in that $^2H1$ NQCC is ~11 kHz larger in **1** than in **2**; computed asymmetry parameters were small ($\eta(^2H1)_\alpha = 0.017$, $\eta(^2H1)_\beta = 0.035$). This behavior correlates with C1–H1 bond length, which is computed to be ~0.01 Å longer in **2** (Table 4). This difference is apparently due to $n_{O5} \rightarrow \sigma^*_{C1,H1}$ donation by the O5 lone-pair anti to the C1–H1 bond in **2**, which induces contraction of the C1–O5 bond and lengthening of the C1–H1 bond. This donation is not possible in **1**. The C1–H1 bond length difference computed in **1** and **2** is also consistent with observed $^1J_{C1,H1}$ values in D-aldopyranoses (*32*), where coupling is ~10 Hz larger for equatorial anomeric protons; the shorter equatorial C–H bond translates into greater *s* character and hence larger $^1J_{CH}$. Differences in ^2H NQCC between anomers at nonanomeric sites in **1** and **2** are considerably smaller, again in agreement with experiment. Computed ^2H NQCC values at each methine carbon are slightly larger for axial ^2H than for equatorial ^2H, an effect that correlates with C–H bond length.

It is noteworthy that the DFT-computed $^2H5$ NQCC is ~5 kHz larger in **1** than in **2** (Table 4). Only one case was examined experimentally (D-[5-^2H]glucose), where a difference of 1.7 kHz was observed (Table 3), with the α-pyranose exhibiting the larger value, in agreement with the DFT computations. Interestingly, the axial $^2H3$ also shows a small difference in NQCC between **1** and **2**; this difference is also observed between *gluco* anomers (Table 3). These effects are attributed to slightly shorter C3–$^2H3$ and C5–$^2H5$ bonds in the

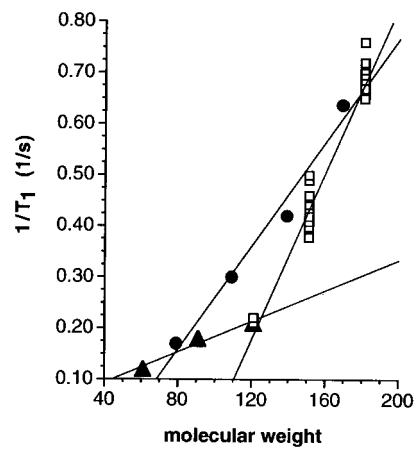

FIG. 3. The dependence of ^{13}C spin–lattice relaxation rate (T_1^{-1}) on molecular weight for (open squares) cyclic (furanose, pyranose), (solid triangles) acyclic aldehyde, and (solid circles) acyclic hydrate forms (data taken from Table 1).

TABLE 2
^{2}H Spin–Lattice Relaxation Times[a] in Various Carbohydrates

Compound	α-pyranose	β-pyranose	α-furanose	β-furanose
D-galactose				
D1	0.0751 ± 0.0007	0.0788 ± 0.0003		
D2	0.072 ± 0.001	0.0726 ± 0.0005		
D-glucose				
D1	$0.068_2 \pm 0.001_6$	0.0774 ± 0.0008		
D2	0.0713 ± 0.0006	0.0704 ± 0.0005		
D3	0.0707 ± 0.0008	0.0714 ± 0.0003		
D5	0.0742 ± 0.0006	0.0755 ± 0.0005		
D-mannose				
D1	0.0686 ± 0.0003	0.0796 ± 0.0009		
D-arabinose				
D1	0.1223 ± 0.0007	0.1187 ± 0.0006		
D2	0.1103 ± 0.0006	0.1082 ± 0.0005		
D-lyxose				
D1	0.0983 ± 0.0003	0.1191 ± 0.0004		
D-ribose				
D1	0.1262 ± 0.0003	0.1221 ± 0.0007	$0.128_1 \pm 0.002_6$	$0.112_5 \pm 0.001_8$
D2	0.1313 ± 0.0006	0.1126 ± 0.0003	$0.130_3 \pm 0.002_9$	$0.109_0 \pm 0.001_8$
D-xylose				
D1 (exp 1)	$0.098_4 \pm 0.001_0$	0.1181 ± 0.0004		
D1 (exp 2)	$0.098_5 \pm 0.001_2$	0.1180 ± 0.0007		
D2	$0.111_0 \pm 0.001_4$	0.1068 ± 0.0005		
DL-glyceraldehyde				
D1	$0.45_0 \pm 0.01_7$[b]	0.1682 ± 0.0009[c]		

[a] In seconds.
[b] Aldehyde.
[c] Hydrate.

α-pyranose, induced by a 1,4-lone-pair effect involving O1 (*33*), which causes a reduction in the computed ^{2}H NQCC.

These theoretical findings are consistent with neutron diffraction crystallographic data reported for methyl α-D-galactopyranoside **6** and methyl β-D-galactopyranoside **7** (*34*). For **6**, $r_{C1–H1}$, $r_{C3–H3}$, and $r_{C5–H5}$ are 1.095, 1.097, and 1.100 Å, respectively, whereas for **7**, the respective bond lengths are 1.104, 1.106, and 1.106 Å. As a control, $r_{C4–H4}$ are identical in **6** and **7** (1.104 Å). The C1–H1 bond is shorter in **6** by an amount (0.009 Å) similar to that predicted from the DFT calculations (Table 4), thereby providing experimental evidence for the reliablity of the theoretical calculations on models **1** and **2** and reinforcing the above conclusions about the dependence of ^{2}H1 NQCC on aldopyranose anomeric configuration.

While the theoretical ^{2}H NQCC values in Table 4 are not in quantitative agreement with experimental data (Table 3), the *trends* exhibited are in good agreement with experiment. The computed 11 kHz difference between ^{2}H1 NQCC in **1** and **2** is nearly identical to that determined experimentally (~11 kHz) if a difference of 0.01 Å in $r_{C1–H1}$ is assumed in the calculations. Overall, these results support the conclusion that ^{2}H1 NQCC values depend on aldopyranose anomeric configuration.

Given the important role of $r_{C–^2H}$ in affecting ^{2}H NQCC values (Fig. 4), it is important to appreciate that these bond lengths will be significantly affected by vicinal lone-pair (*35*), 1,3-lone-pair (*36*), and 1,4-lone-pair (*33*) effects in saccharides. Thus, for example, rotation of C–O bonds on carbons bearing deuterons changes the disposition of oxygen lone-pairs with respect to the C–^{2}H bond, thereby changing its length and, indirectly, affecting the magnitudes of $^1J_{CH}$ and ^{2}H NQCC values. At anomeric carbons, C–O bond conformation is controlled by stereoelectronic factors which are absent at other C–O bonds in saccharides. These differences may account, in part, for the observed dependence of ^{2}H NQCC on anomeric configuration; anomeric C–O bonds are equally constrained in both anomers, thereby reducing the effects of C–O bond rotational averaging on the coupling and accentuating the difference in ^{2}H NQCC.

D-Xylopyranoses show the same NQCC behavior as D-glucopyranoses, that is, NQCC for ^{2}H1 depends on anomeric configuration. Interestingly, ^{2}H1 NQCC is larger in β-D-arabinopyranose than in α-D-arabinopyranose, in contrast to observations made in D-Gal, D-Glc, D-Man, and D-Xyl (Table 3). This result is expected, however, since the preferred ring conformation assumed by D-arabinopyranoses is $^1C_4$ in which an axial C1–H1 bond occurs in the α-pyranose and an equatorial C1–H1 bond occurs in the β-pyranose (Scheme 1). ^{2}H NQCC values for ^{2}H2 in D-xylopyranoses and D-arabinopyranoses are essentially unaffected by anomeric configuration.

TABLE 3
^{2}H Nuclear Quadrupolar Coupling Constants (NQCC)[a] in Various Carbohydrates

Compound	α-pyranose	β-pyranose	α-furanose	β-furanose
D-galactose				
C1–D1	175.8	173.5		
C2–D2	178.8	178.5		
D-glucose				
C1–D1	178.9	173.1		
C2–D2	178.6	178.1		
C3–D3	178.6	177.4		
C5–D5	175.7	174.0		
D-mannose				
C1–D1	176.5	172.2		
D-arabinose				
C1–D1	172.2	174.0		
C2–D2	176.9	177.9		
D-lyxose				
C1–D1	178.4	173.7		
D-ribose				
C1–D1	174.1	171.1	173.0	176.8
C2–D2	176.0	175.8	173.6	177.9
D-xylose				
C1–D1	176.8	171.5		
C2–D2	176.3	177.3		
DL-glyceraldehyde				
C1–D1	139.2[b]	175.6[c]		

[a] In kHz ± 1 kHz.
[b] Aldehyde.
[c] Hydrate.

TABLE 4
Theoretical ^{2}H NQCC Values in 1 and 2 From *Ab initio* Calculations

Bond	Bond length (Å)	Computed ^{2}H NQCC (kHz)
1		
C1–H1 eq	1.0986 (**−0.0113**)[a]	187.3 (**11.3**)[a]
C2–H2 ax	1.0974 (0.0007)	196.0 (−0.3)
C2–H2 eq	1.0955 (−0.0004)	198.2 (0.0)
C3–H3 ax	1.0969 (**−0.0030**)	196.0 (**1.6**)
C3–H3 eq	1.0966 (0.0005)	198.4 (−0.3)
C4–H4 ax	1.0985 (0.0009)	195.6 (−0.5)
C4–H4 eq	1.0977 (0.0000)	197.3 (0.0)
C5–H5 ax	1.0992 (**−0.0055**)	190.5 (**4.7**)
C5–H5 eq	1.0940 (0.0000)	197.1 (0.2)
2		
C1–H1 ax	1.1099	176.0
C2–H2 ax	1.0967	196.3
C2–H2 eq	1.0959	198.2
C3–H3 ax	1.0999	194.4
C3–H3 eq	1.0961	198.7
C4–H4 ax	1.0976	196.1
C4–H4 eq	1.0977	197.3
C5–H5 ax	1.1047	185.8
C5–H5 eq	1.0940	196.9

[a] Value in parentheses is the difference in bond length or NQCC ($Value_1$–$Value_2$).

^{2}H1 NQCC values in D-lyxopyranoses and D-ribopyranoses are larger in the α-pyranose, but these results are difficult to interpret due to the presence of conformational averaging (i.e., these aldopyranoses exist as a mixture of interconverting chair forms in solution).

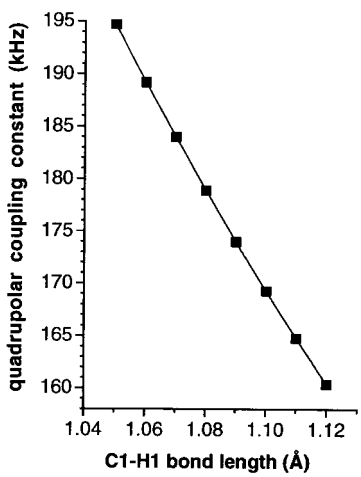

FIG. 4. Dependence of calculated ^{2}H1 NQCC values (Eq. [3]) on C1–H1 bond length in α-D-glucopyranose.

In contrast to behavior observed in aldopyranoses, ^{2}H NQCC values for ^{2}H1 and ^{2}H2 in D-ribofuranoses are nearly equally affected by anomeric configuration, in contrast to observations made in conformationally rigid aldopyranose rings. This behavior is attributed to the significantly different ring conformations assumed by the α- and β-furanoses in solution, which cause the C1–^{2}H1 and C2–^{2}H2 bonds to assume different orientations in the two aldofuranose anomers. To examine this effect further, ^{2}H NQCC values for the ring C–^{2}H bonds were calculated in the model aldofuranose, 2-deoxy-β-D-*erythro*-pentofuranose **3**, using DFT-optimized geometries reported previously (*29*). Theoretical NQCC values vary with ring conformation (Fig. 5A) in a manner similar to that observed previously for the corresponding $^1J_{CH}$ values (Fig. 5B), demonstrating the importance of $r_{C-H/^2H}$ in dictating the magnitudes of both the scalar and quadrupolar couplings. These results suggest that ^{2}H NQCC values, like $^1J_{CH}$ (*35*), may be useful probes of aldofuranosyl ring conformation in solution and thus deserve further scrutiny.

CONCLUSIONS

The primary aim of this investigation was to determine ^{2}H NQCC values for deuterium nuclei at different positions and environments in saccharides. These values were determined indirectly through measurements of ^{13}C and ^{2}H spin–lattice relaxation times in site-specific ^{13}C- and ^{2}H-labeled compounds. In order to minimize sources of error, the measure-

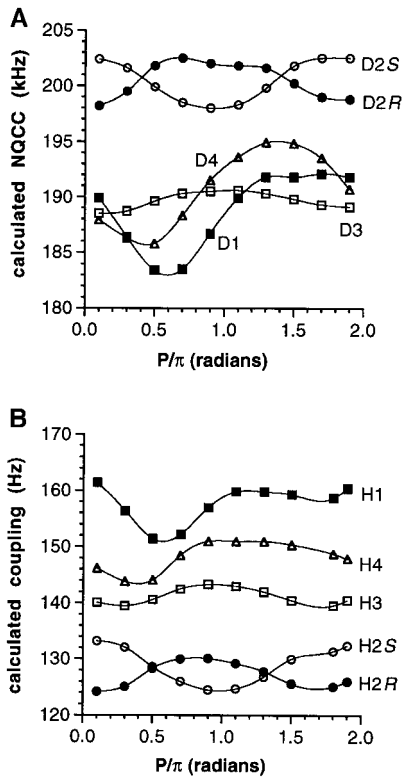

FIG. 5. (A) Calculated ^{2}H NQCC values from density functional theory (B3LYP/6-31G* geometries and B3LYP/[5*s*2*p*1*d*,3*s*1*p*] for NQCC calculations) in **3** as a function of ring conformation. Calculations were restricted to the 10 envelope conformations, where ^3E = 0.1 P/π, E_4 = 0.3 P/π, and so forth, and to one set of exocyclic hydroxymethyl and C–O conformations; see Ref. (*29*) for structural details. Calculated asymmetry parameters, η, for all of the calculated couplings ranged from 0.006 to 0.054. (B) Calculated $^1J_{CH}$ in **3** from density functional theory (B3LYP/6-31G* geometries and B3LYP/[5*s*2*p*1*d*,2*s*] for $^1J_{CH}$ calculations) (data taken from Ref. (*29*)).

ments were made on solutions containing equimolar concentrations of the saccharide singly labeled with ^{13}C and ^{2}H at the same site in the molecule. The ^{2}H T_1 measurements were simplified by conducting measurements in ^{2}H-depleted ^1H_2O solvent (anomeric ^{2}H signals sometimes overlap with the HO^{2}H signal). Thus, an underlying assumption is that contributions made to ^{13}C T_1 relaxation by solvent water protons and/or by the presence of carbon-bound and/or hydroxyl protons in the vicinity of the labeled carbon are negligible; that is, we assume that the dominant source of relaxation of the ^{13}C nucleus derives from its directly attached proton.

Other experimental methods are available for the determination of ^{2}H NQCC values. Studies of single crystals and powders by wide-line NMR methods yield quadrupolar coupling constants directly in the solid state (*1*). In solution, Hardy *et al.* (*37*) described recently a relaxation method to determine ^{2}H NQCC values in ^{13}C–^{2}H fragments involving measurements of ^{2}H and ^{13}C T_1 and steady-state ^{13}C NOE measurements under ^{2}H saturation in a single deuterated sample. In principle, solid-state NMR studies provide the most definitive measurements, and, given the uncertainties of solution ^{2}H NQCC determinations caused by the effect of C–H/^{2}H bond length, it would be valuable to prepare single crystals or polycrystalline samples of anomeric [^{2}H]aldopyranosides to test the conclusions drawn from the present data.

The experimentally determined ^{2}H NQCC values (Table 3) fall within the expected range; they are commonly assumed to be ~170 kHz in carbohydrates and are generally considered to be independent of structure (*38*). The present results, however, contradict the latter assumption. ^{2}H NQCC for ^{2}H1 depends on anomeric configuration in aldopyranoses, whereas the sensitivity of ^{2}H NQCC at nonanomeric carbons to anomeric configuration in these rings is much reduced, presumably due in part to the effect of C–O conformational averaging on C–^{2}H bond lengths. In contrast, all ring ^{2}H NQCC values may be influenced by anomeric configuration in aldofuranosyl rings due to their inherent conformational flexibility. These conclusions are supported by theoretical (DFT) calculations of ^{2}H NQCC in model aldopyranoses and aldofuranoses, which suggest that the effect is grounded largely in variations in C–H(^{2}H) bond lengths between structures caused by differential oxygen lone-pair effects. It should be appreciated, however, that the effect of C–O bond torsional averaging in solution will modulate ^{2}H NQCC values due to vicinal lone-pair effects (*35*) on C–^{2}H bond lengths, leading to smaller differences than predicted theoretically. Likewise, small librational fluctuations in α- and β-pyranose rings could also yield smaller experimental differences between anomers than predicted by theory.

Given the dominant role of local structure and geometry in dictating their magnitudes, ^{2}H NQCC values obtained on monosaccharides in this study can be applied with reasonable confidence to studies of oligosaccharides containing these residues. Knowledge of the structural dependencies of these couplings will be essential to the accurate interpretation of ^{2}H relaxation data in terms of molecule motion and dynamics in solution.

ACKNOWLEDGMENTS

This work was supported by a grant from Omicron Biochemicals, Inc. of South Bend, IN and by the Office of Basic Energy Sciences of the U.S. Department of Energy. This is Document No. NDRL-4143 from the Notre Dame Radiation Laboratory.

REFERENCES

1. H. H. Mantsch, H. Saito, and I. C. P. Smith, Deuterium magnetic resonance, applications in chemistry, physics and biology, *Prog. NMR Spectrosc.* **11,** 211–271 (1977).
2. D. R. Muhandiram, T. Yamazaki, B. D. Sykes, and L. E. Kay, Measurement of ^{2}H T_1 and $T_{1\rho}$ relaxation times in uniformly ^{13}C-labeled and fractionally ^{2}H-labeled proteins in solution, *J. Am. Chem. Soc.* **117,** 11536–11544 (1995).
3. D. Yang, A. Mittermaier, Y. K. Mok, and L. E. Kay, A study of protein side-chain dynamics from new ^{2}H auto-correlation and ^{13}C cross-

correlation NMR experiments: Application to the N-terminal SH3 domain from drk, *J. Mol. Biol.* **276,** 939–954 (1998).

4. J. R. Lyerla, Jr., and G. C. Levy, Carbon-13 nuclear spin relaxation, *in* "Topics in Carbon-13 NMR Spectroscopy," Vol. 1, pp. 79–148, Wiley, New York (1974).
5. T. Chiba, Deuteron magnetic resonance study of some crystals containing an O–D···O bond, *J. Chem. Phys.* **41,** 1352–1358 (1964).
6. R. Bersohm, Field gradients at the deuteron in molecules, *J. Chem. Phys.* **32,** 85–88 (1960).
7. M. Dixon, T. A. Claxton, and R. E. Overill, The dependence of the deuteron quadrupolar coupling constant, diamagnetic shielding, and diamagnetic susceptibility of methane on internuclear distance, *J. Magn. Reson.* **12,** 193–198 (1973).
8. A. S. Serianni, H. A. Nunez, and R. Barker, Carbon-13-enriched carbohydrates. Preparation of aldononitriles and their reduction with a palladium catalyst, *Carbohydr. Res.* **72,** 71–78 (1979).
9. A. S. Serianni, T. Vuorinen, and P. B. Bondo, Stable isotopically-enriched D-glucose: Strategies to introduce carbon, hydrogen and oxygen isotopes at various carbons, *J. Carbohydr. Chem.* **90,** 513–541 (1990).
10. A. S. Serianni and P. B. Bondo, ^{13}C-labeled D-ribose: Chemienzymic synthesis of various isotopomers, *J. Biomol. Struct. Dynam.* **11,** 1133–1148 (1994).
11. A. S. Serianni, E. L. Clark, and R. Barker, Carbon-13-enriched carbohydrates. Preparation of erythrose, threose, glyceraldehyde and glycolaldehyde with ^{13}C-enrichment in various carbon atoms, *Carbohydr. Res.* **72,** 79–91 (1979).
12. A. S. Serianni, E. Cadman, J. Pierce, M. L. Hayes, and R. Barker, Enzymic synthesis of ^{13}C-enriched aldoses, ketoses, and their phosphate esters, *Methods Enzymol.* **89,** Part D, 83–92 (1982).
13. A. S. Serianni and R. Barker, Isotopically enriched carbohydrates: The preparation of [^{2}H]-enriched aldoses by catalytic hydrogenolysis of cyanohydrins with $^2H_2$, *Can. J. Chem.* **57,** 3160–3167 (1979).
14. A. S. Serianni, E. L. Clark, and R. Barker, Chemical synthesis of aldoses enriched with isotopes of hydrogen and oxygen, *Methods Enzymol.* **89,** Part D, 79–83 (1982).
15. R. L. Vold, J. S. Waugh, M. P. Klein, and D. E. Phelps, Measurement of spin relaxation in complex systems, *J. Chem. Phys.* **48,** 3831–3832 (1968).
16. G. H. Weiss and J. A. Ferretti, Optimal design of relaxation time experiments, *Prog. NMR Spectrosc.* **4,** 317–335 (1988).
17. H. Saito, H. H. Mantsch, and I. C. P. Smith, Correlation between deuterium and carbon-13 relaxation times. A convenient means to determine the mechanism of ^{13}C relaxation and ^{2}H quadrupolar coupling constants, *J. Am. Chem. Soc.* **95,** 8453–8455 (1973).
18. J. M. Berry, L. D. Hall, D. G. Welder, and K. F. Wong, Proton spin–lattice relaxation: A new, quantitative measure of aglycone–sugar interactions, *in* "Anomeric Effect: Origin and Consequences" (W. A. Szarek and D. Horton, Eds.), ACS Symposium Series 87, pp. 30–49, American Chemical Society (1979).
19. P. Dais, Carbon-13 nuclear magnetic relaxation and motional behavior of carbohydrate molecules in solution, *Adv. Carbohydr. Chem. Biochem.* **51,** 63–131 (1995).
20. I. Carmichael, *Ab initio* quadratic configuration interaction calculation of indirect NMR spin–spin coupling constants, *J. Phys. Chem.* **97,** 1789–1792 (1993).
21. M. J. Frisch, G. W. Trucks, H. B. Schlegel, P. M. W. Gill, B. G. Johnson, M. A. Robb, J. R. Cheeseman, T. Keith, G. A. Petersson, J. A. Montgomery, K. Raghavachari, M. A. Al-Laham, V. G. Zakrzewski, J. V. Ortiz, J. B. Foresman, C. Y. Peng, P. Y. Ayala, W. Chen, M. W. Wong, J. L. Andres, E. S. Replogle, R. Gomperts, R. L. Martin, D. J. Fox, J. S. Binkley, D. J. Defrees, J. Baker, J. P. Stewart, M. Head-Gordon, C. Gonzalez, and J. A. Pople, "Gaussian 94," Gaussian, Inc., Pittsburgh (1995).
22. A. D. Becke, Density-functional thermochemistry. III. The role of exact exchange, *J. Chem. Phys.* **98,** 5648–5652 (1993).
23. J. C. Slater, "The Self-Consistent Field for Molecules and Solids," McGraw–Hill, New York (1974).
24. A. D. Becke, Density functional theories in quantum chemistry—Beyond the local density approximation, *in* "ACS Symposium Series 394," pp. 165–179, American Chemical Society, Washington, DC (1989).
25. S. H. Vosko, L. Wilk, and M. Nusair, Accurate spin-dependent electron liquid correlation energies for local spin density calculations: A critical analysis, *Can. J. Phys.* **58,** 1200–1211 (1980).
26. C. Lee, W. Yang, and R. G. Parr, Development of the Colle–Salvetti correlation-energy formula into a functional of the electron density, *Phys. Rev. B* **37,** 785–789 (1988).
27. W. J. Hehre, R. Ditchfield, and J. A. Pople, Self-consistent molecular orbital methods. XII. Further extensions of gaussian-type basis sets for use in molecular orbital studies of organic molecules, *J. Chem. Phys.* **56,** 2257–2261 (1972).
28. E. Juaristi and G. Cuevas, "The Anomeric Effect," CRC Press, Boca Raton (1995).
29. F. Cloran, I. Carmichael, and A. S. Serianni, ^{13}C–^{1}H and ^{13}C–^{13}C spin-coupling behavior in aldofuranosyl rings from density functional theory, *J. Phys. Chem. A* **103,** 3783–3785 (1999).
30. M. F. Czarniecki and E. R. Thornton, Carbon-13 nuclear magnetic resonance of ganglioside sugars. Spin–lattice relaxation probes for structure and microdynamics of cell surface carbohydrates, *J. Am. Chem. Soc.* **99,** 8279–8282 (1977).
31. A. S. Serianni and R. Barker, ^{13}C spin–lattice relaxation times of [1-^{13}C]-enriched carbohydrates, *J. Magn. Reson.* **49,** 335–340 (1982).
32. K. Bock, I. Lundt, and C. Pedersen, Assignment of anomeric structure to carbohydrates through geminal ^{13}C-H coupling constants, *Tetrahedron Lett.* **13,** 1037–1040 (1973).
33. F. Cloran, Y. Zhu, J. Osborn, I. Carmichael, and A. S. Serianni, 2-deoxy-β-D-ribofuranosylamine: Quantum mechanical calculations of molecular structure and NMR spin–spin coupling constants in nitrogen-containing saccharides, *J. Am. Chem. Soc.,* in press.
34. S. Takagi and G. A. Jeffrey, Neutron diffraction refinement of the crystal structures of methyl α-D-galactopyranoside monohydrate and methyl β-D galactopyranoside, *Acta Crystallogr. Sect. B* **35,** 902–906 (1979).
35. A. S. Serianni, J. Wu, and I. Carmichael, One-bond ^{13}C–^{1}H spin-coupling constants in aldofuranosyl rings: Effect of conformation on coupling magnitude, *J. Am. Chem. Soc.* **117,** 8645–8650 (1995).
36. J. Kennedy, J. Wu, K. Drew, I. Carmichael, and A. S. Serianni, Carbohydrate reaction intermediates: Effect of ring-oxygen protonation on the structure and conformation of aldofuranosyl rings, *J. Am. Chem. Soc.* **119,** 8933–8945 (1997).
37. E. H. Hardy, R. Witt, A. Dölle, and M. D. Zeidler, A new method for the determination of the dynamic isotope effect and the deuterium quadrupole coupling constant in liquids, *J. Magn. Reson.* **134,** 300–307 (1998).
38. W.-C. Huang, J. Orban, A. Kintanar, B. R. Reid, and G. P. Drobny, A solid-state deuterium NMR study of furanose ring dynamics in [d(CGCGAATTCGCG)]$_2$, *J. Am. Chem. Soc.* **112,** 9059–9068 (1990).